This journal is © The Royal Society of Chemistry 2014

Electronic supplementary information (SI):

SI-Experimental procedures

All substances used in this study were analytical grade and without further purification. Deionized water was used in all experiments.

Synthesis of materials: The g-C_3N_4 powder was synthesized by heating melamine in an alumina combustion boat to 500 ºC at a heating rate of 10ºC /min for 4 h under a argon gas flow (20mL/min), followed by 4 h at that temperature prior to cooling. Phosphoric acid modified g-C_3N_4 was synthesized by mixing of as prepared g-C_3N_4 and different amount of phosphate. In a typical synthesis procedure, 0.5 g g-C_3N_4 powders were impregnated in a 20 mL of planned-concentration ortho-phosphoric acid solution (or sulfuric acid and hydrofluoric acid) by stirring for 2 h. Subsequently, the suspension was dried at 100 ºC, along with the thermal treatment at 450 ºC for 1 h. The phosphoric acid modified samples are defined as XP-CN, in which P means phosphoric acid, CN is used to represent g-C_3N_4 and X indicates the theoretical molar percent ratio of phosphorus atoms to nitrogen atoms.

Characterization of materials: The samples were characterized by X-ray Diffraction (XRD) with a Rigaku D/MAX-rA diffractometer (Japan), using CuKα radiation (α= 0.15418 nm), and an accelerating voltage of 30 kV and an emission current of 20 mA were employed. X-ray Photoelectron Spectroscopy (XPS) measurements were performed in a Kratos-AXIS ULTRA DLD spectrometer equipped with Al (Mono) X-ray source, and all the binding energies were calibrated to the C1s peak at 284.6 eV. The morphology of the samples were determined by a JEOL JEM-2010 transmission electron microscope (TEM) operated at 200 kV. The ultraviolet-visible (UV-Vis) absorption spectra of the samples were recorded with a Model Shimadzu UV-2550 spectrophotometer. Fourier transform infrared spectra (FTIR) were obtained on a Spectrum One at the range of 500-4000 cm^{-1} using KBr as a dilute. Thermogravimetric (TG) analysis was carried out with an SDTQ600 apparatus in a flow of air (20 mL/min) at a heating rate of 10 °C/min.

The steady-state surface photovoltage spectroscopy (SPS) measurements of samples were conducted with a home-built apparatus with a lock-in amplier (SR830) synchronized with a light chopper (SR540). The powder sample was sandwiched between two ITO glass electrodes by which the outer electric field could be employed. The sandwiched electrodes could be arranged in an atmosphere-controlled container with a quartz window and mono-chromatic light was obtained by passing light from a 500W xenon lamp (CHF XQ500W) through a double prism monochromator (SBP300).

Time-resolved surface photovoltage (TR-SPV) measurements of samples were operated by the process that the sample chamber connected an ITO glass as top electrode and a steel substrate as bottom electrode, and a 10 μm thick mica spacer was placed between the ITO glass and the sample to decrease the space charge region at the ITO-sample interface. The samples were excited by a radiation pulse of 355 nm with 10 ns width from a second harmonic Nd: YAG laser (Lab-130-10H, Newport, Co.). Intensity of the pulse was measured by a high energy pyroelectric sensor (PE50BF-DIF-C, Ophir Photonics Group). The signals were amplified with a preamplier and then registered by a 1 GHz digital phosphor oscilloscope (DPO 4104B, Tektronix). The TR-SPV measurements were performed in air atmosphere and at room temperature.

Temperature-programmed desorption (TPD) of oxygen was conducted with a home-built apparatus. In a typical O_2-TPD experiment, 30 mg of the powder sample was pretreated in a Pyrex tube (i.d. 6 mm) at 270 ºC for 30 min by an ultra-high-pure He flow. After the treatment, the

temperature was cooled to room temperature. For O_2 adsorption saturation, the sample was continuously blown with ultra-high-pure O_2 for 2h at room temperature. Subsequently, the sample was blown with the ultra-high-purity He flow for removal of residual O_2 in the quartz tube and a small part of O_2 physically adsorbed on the sample. After that, the O_2-TPD profile of the sample was recorded with increasing the temperature from room temperature to 600 ℃ at a heating rate of 10 ℃/min under 20mL/min of ultra-high-purity He flow. The desorbed O_2 was analyzed by a gas chromatograph (GC-2014, SHIMADZU) with a TCD detector. The corrected O_2-TPD curves were obtained by subtracting the corresponding N_2-TPD value from the original O_2-TPD one.

Photoelectrochemical experiments were performed in three-electrode cell with a Platinum plate (99.9%) as the counter electrode, and a saturated KCl Ag/AgCl electrode (SSE) as the reference electrode on a LK2006A workstation. The working electrode (illumination area is about 0.5 cm^2), was positioned in a 0.5 M $NaClO_4$ electrolyte with the FTO side facing the incident light. High-purity O_2 gas was used to bubble through the electrolyte before and during the electrochemical O_2 reduction experiments. The photoelectrodes were prepared as follows: Firstly, the paste was prepared by grinding 10 mg of g-C_3N_4 and 200 μL of ethanol.Then the paste was coated on the conductive tape sticked on the FTO. Finally, the FTO glass substrate were dried in air at 80 ℃ for 30min.

Photocatalytic experiments: The photocatalytic activities of the samples were tested by degrading liquid-phase phenol and gas-phase aldehyde under light irradiation, respectively. A 150 W Xenon lamp was chosen as a light source. In a typical liquid-phase photocatalytic experiment, 0.1 g of photocatalyst and 20 mL of 10 mg/L phenol aqueous solution were mixed by stirring for 1h in an open glass reactor under light irradiation. The distance between the light source and the reactor was 10 cm. After centrifugation, the phenol concentrations were analyzed by the 4-aminoantipyrine spectrophotometric method at the characteristic optical adsorption (510 nm) of phenol with a Shimadzu UV-2550 spectrophotometer.

Gas-phase photocatalytic experiment was performed in a 640 mL of cylindrical quartz reactor with three mouths for introducing desired-amount of photocatalyst powders and planned-concentration of acetaldehyde gas. The reactor was placed horizontally and irradiated from the top side by using a 150 W Xenon lamp. In a typical photocatalytic process, 0.1 g of photocatalyst was used, and a pre-mixed gas system, in which contained 810 ppm of acetaldehyde, 20% of O_2 and 80% of N_2, was introduced into the reactor. To reach adsorption saturation, the mixed gas was continuously flew past the reactor for 30 min prior to the irradiation. The acetaldehyde concentrations at different time intervals in the photocatalysis system were measured by a gas chromatograph (GC-2014, SHIMADZU) equipped with a flame ionization detector.

SI-Figures

SI-figure 1 XRD patterns (A) DRS spectra (B) and FTIR spectra (C) of CN and XP-CN.

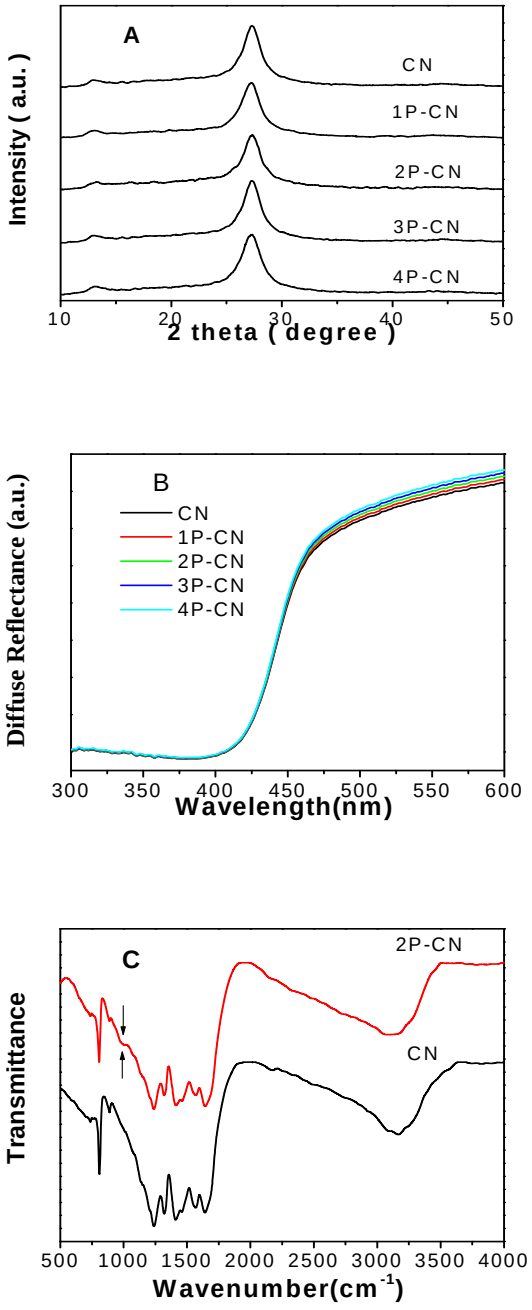

For the FTIR spectra of CN and 2P-CN shown in SI-figure 1 C, the peaks at 1241, 1322, 1406 and 1571 cm^{-1} result from the typical stretching modes of CN heterocycles. And the characteristic breathing mode of triazine units are observed at 806 cm^{-1} [4e,4i]. For the FTIR peaks at about 1630 and 3165 cm^{-1}, they are ascribed to the adsorbed surface hydroxyls and water molecules. Interestingly, a new FTIR peak for 2P-CN at about 985 cm^{-1} is seen, attributed to the phosphate groups. Thus, it is confirmed that the phosphate groups are modified on the surfaces of CN, and no other functional groups are introduced.

SI-figure 2 XPS spectra of CN and XP-CN, C1s (A), N1s (B), O1s (C), and P2p (D).

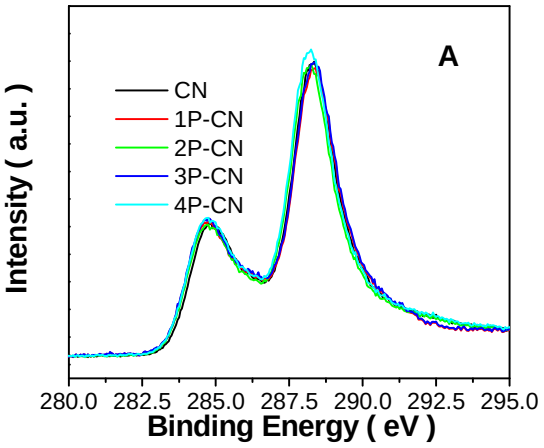

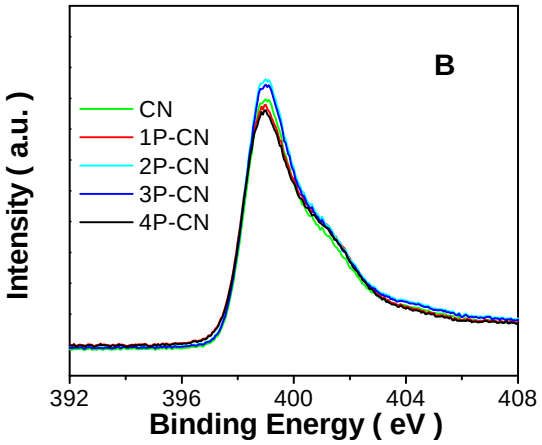

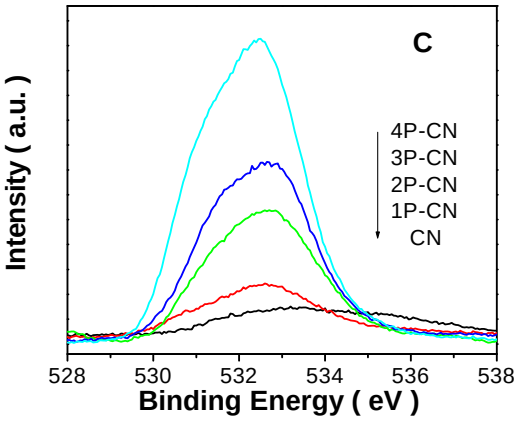

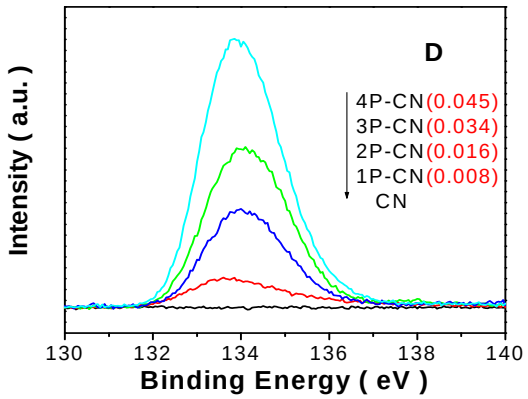

SI-figure 3 SS-SPS responses of CN (A) and 2P-CN (B) in different atmospheres.

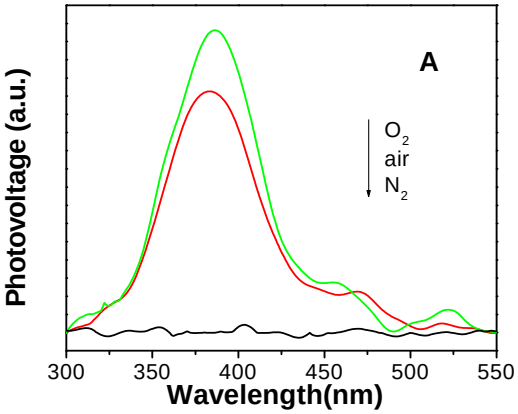

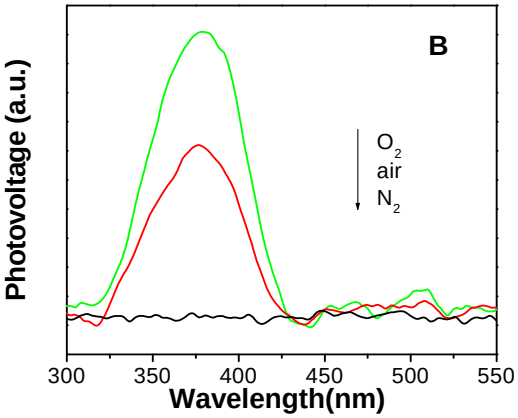

SI-figure 4 The first-order kinetic plots of CN and 2P-CN in the different-concentration phenol solutions ((a: 2P-CN, 10 mg/L; b: CN, 10 mg/L; c: 2P-CN, 20 mg/L; d: CN, 20 mg/L) (A)), and that of CN and 2P-CN in different O_2-bubbled systems ((a: 2P-CN, O_2; b: 2P-CN, air; c: CN, O_2; d: CN, air) (B)).

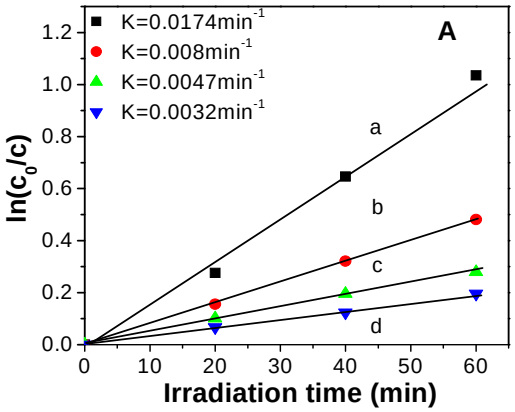

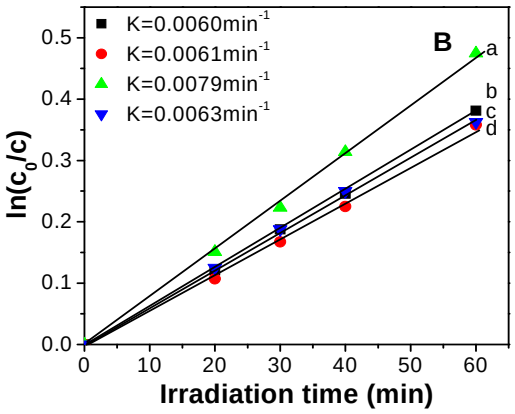

From the kinetic-order plots shown in SI-figure 4A, one can see that the 2P-CN displays better photocatalytic performance than CN for phenol degradation. In SI-figure 4b, the photocatalytic activity of 2P-CN is enhanced greatly in the O_2-bubbled system, while that of CN is nearly unchanged. This implies that the modified phosphate could be favorable for O_2 adsorption so as to promote the separation of photogenerated charge carriers of g-C_3N_4. In addition, it is confirmed that all photocatalytic degradation reactions follow pseudo-first order kinetic.

SI-figure 5 TG curves of CN and 2P-CN.

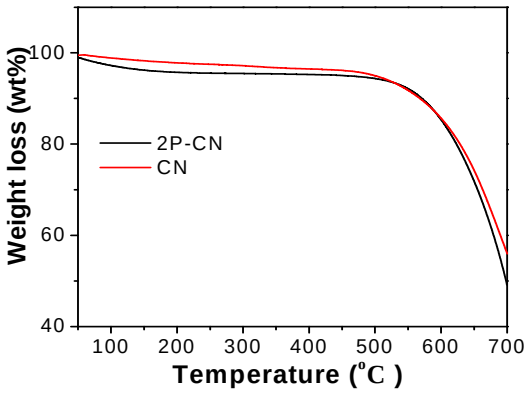

SI-figure 6 XRD patterns of 2Y-CN (A), the CN means the pure g-C_3N_4, Y means different acid and 2 means theoretical molar percent ratio of sulphur (or fluorine) atom to nitrogen one is 2%.

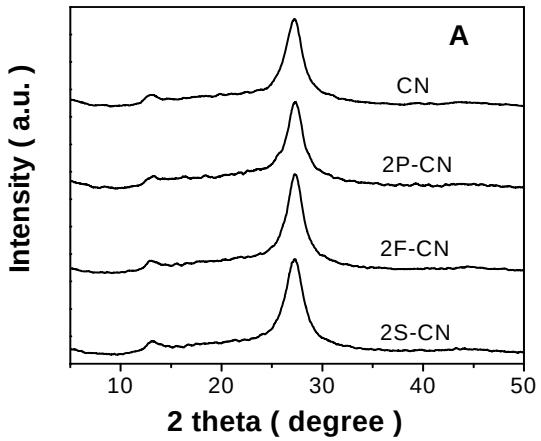

SI-figure 6 XPS spectra (B) (a) S2p and (b) F1s of 2S-CN and 2F-CN, respectively.

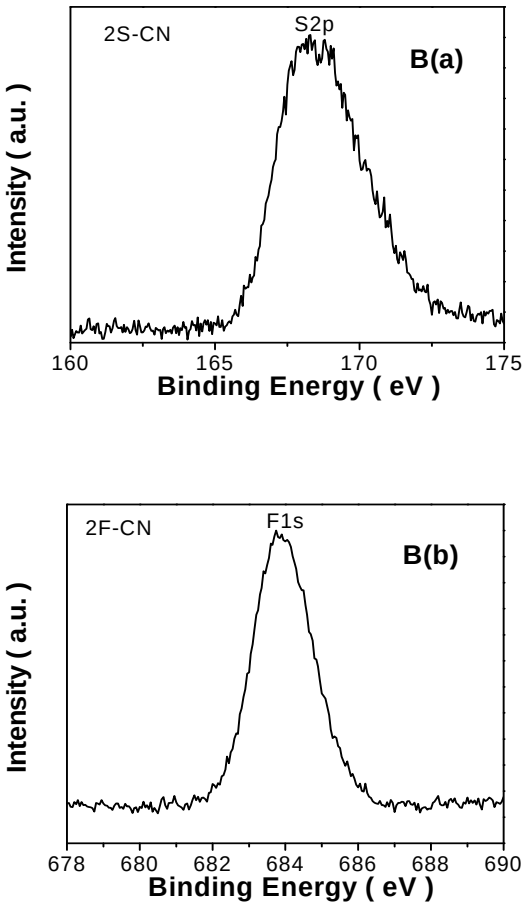

SI-figure 6 Curves of corrected O_2 temperature-programmed desorption of 2Y-CN (C).

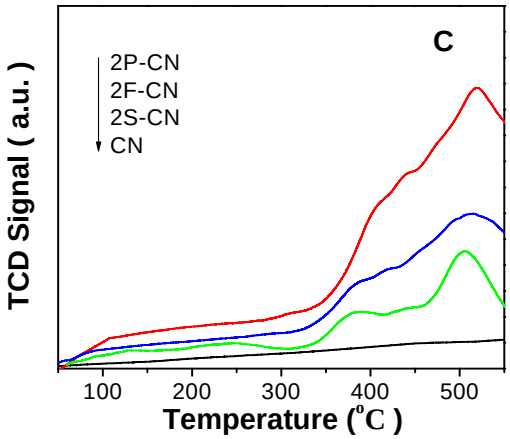

SI-figure 6 SS-SPS (a) and TR-SPV (b) responses of CN and 2Y-CN in air, and the inset indicates DRS spectra of CN and 2Y-CN (D).

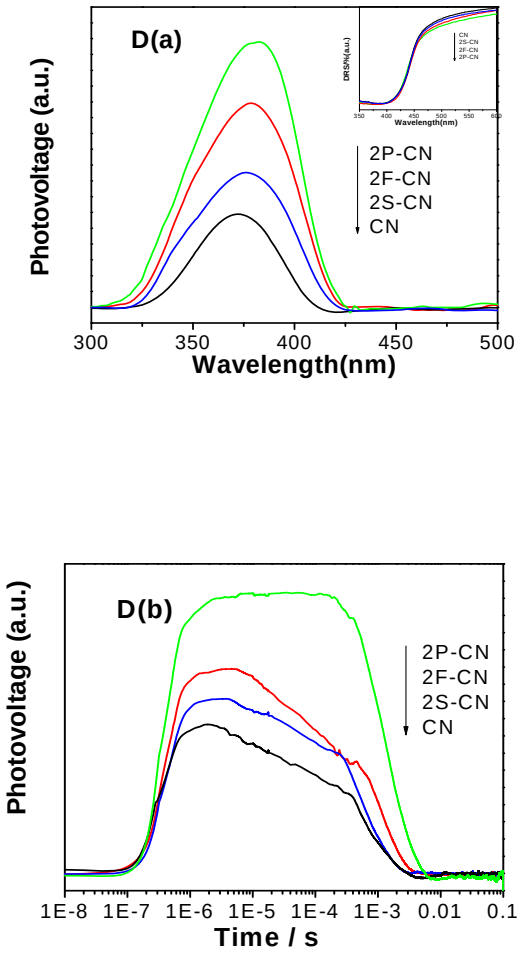

SI-figure 6 Photocatalytic degradation rates of gas-phase acetaldehyde of CN and 2Y-CN (E).